Atmos. Chem. Phys., 18, 14161–14173, 2018
https://doi.org/10.5194/acp-18-14161-2018
© Author(s) 2018. This work is distributed under
the Creative Commons Attribution 4.0 License.

Atmospheric Chemistry and Physics
Open Access
EGU

Measurements of NO and NO_2 exchange between the atmosphere and *Quercus agrifolia*

Erin R. Delaria[1], **Megan Vieira**[1], **Julie Cremieux**[2], **and Ronald C. Cohen**[1,3]

[1]Department of Chemistry, University of California Berkeley, Berkeley, CA 94720, USA
[2]Department of Chemistry, Université Pierre et Marie Curie, Paris, France
[3]Department of Earth and Planetary Science, University of California Berkeley, Berkeley, CA 94720, USA

Correspondence: Ronald C. Cohen (rccohen@berkeley.edu)

Received: 1 May 2018 – Discussion started: 31 May 2018
Revised: 14 September 2018 – Accepted: 18 September 2018 – Published: 5 October 2018

Abstract. NO_2 foliar deposition through the stomata of leaves has been identified as a significant sink of NO_x within a forest canopy. In this study, we investigated NO_2 and NO exchange between the atmosphere and the leaves of the native California oak tree *Quercus agrifolia* using a branch enclosure system. NO_2 detection was performed with laser-induced fluorescence (LIF), which excludes biases from other reactive nitrogen compounds and has a low detection limit of 5–50 ppt. We performed both light and dark experiments with concentrations between 0.5 and 10 ppb NO_2 and NO under constant ambient conditions. Deposition velocities for NO_2 during light and dark experiments were 0.123 ± 0.009 and 0.015 ± 0.001 cm s^{-1}, respectively. Much slower deposition was seen for NO, with deposition velocities of 0.012 ± 0.002 and 0.005 ± 0.002 cm s^{-1} measured during light and dark experiments, respectively. This corresponded to a summed resistance of the stomata and mesophyll of 6.9 ± 0.9 s cm^{-1} for NO_2 and 140 ± 40 s cm^{-1} for NO. No significant compensation point was detected for NO_2 uptake, but compensation points ranging from 0.74 to 3.8 ppb were observed for NO. NO_2 and NO deposition velocities reported here are comparable both with previous leaf-level chamber studies and inferences from canopy-level field measurements. In parallel with these laboratory experiments, we have constructed a detailed 1-D atmospheric model to assess the contribution of leaf-level NO_x deposition to the total NO_x loss and NO_x canopy fluxes. Using the leaf uptake rates measured in the laboratory, these modeling studies suggest that loss of NO_x to deposition in a California oak woodland competes with the pathways of HNO_3 and $RONO_2$ formation, with deposition making up 3 %–22 % of the total NO_x loss. Additionally, foliar uptake of NO_x at these rates could account for ∼ 15 %–30 % canopy reduction of soil NO_x emissions.

1 Introduction

Nitrogen oxides ($NO_x \equiv NO + NO_2$) are a group of highly reactive trace gases that control the oxidative capacity of the atmosphere by regulating the amounts of ozone, hydroxyl radicals, volatile organic compounds, and other key atmospheric species (Crutzen, 1979). NO_x is also directly toxic in high concentrations, plays a major role in tropospheric ozone production, and serves as a source of NO_3^-, a key nutrient for ecosystems and a component of acid rain. NO_x is primarily emitted as nitric oxide (NO) through fossil fuel combustion, biomass burning, lightning, and microbial activity in soils (Seinfeld and Pandis, 2006). NO is rapidly oxidized to nitrogen dioxide (NO_2) through reactions with ozone and peroxy radicals, and in the daytime NO_2 subsequently photolyzes to re-form NO. The interconversion of NO and NO_2 reaches steady state within a few minutes during the daytime (Crutzen, 1979). The effects of NO_x on urban chemistry, where anthropogenic emissions dominate the NO_x source, have been extensively studied. However, the processes affecting NO_x in forested and agricultural regions are less well understood.

In forests and agricultural lands, the major source of NO_x is NO emitted as a by-product of microbial denitrification and nitrification (Mckenney et al., 1982; Caranto and Lancaster, 2017). Deposition of NO_2 to plant canopies is thought

to be an important sink of NO_x in forests, substantially reducing the contribution of soil-emitted NO_x to the atmospheric NO_x budget. Jacob and Wofsy (1990) observed low NO_x above the canopy over the Amazon forest during the wet season. Using a 1-D chemical and transport model constrained by observed NO_x and ozone, they concluded that a substantial fraction of soil NO_x must be absorbed by the canopy. Extrapolation of these ideas to forests with different leaf area indices suggest that 20 %–50 % of the global fraction of soil-emitted NO_x is lost to vegetation (Yienger and Levy, 1995; Lerdau et al., 2000). Using the framework of Jacob and Wofsy (1990) and Yienger and Levy (1995), global atmospheric models have been tuned to describe observed atmospheric NO_x concentrations and tropospheric ozone production using a canopy reduction factor (CRF). The CRF is an adjustable parameter that accounts for the difference between soil NO emissions and the amount of NO_x ventilated through the canopy (Yienger and Levy, 1995; Vinken et al., 2014). However, CRFs are implemented in an unphysical manner where they act only on soil NO_x emissions and not on other NO_x present in the plant canopy. An improved understanding is needed of the physical and biochemical processes governing the foliar uptake of NO_x at the ecosystem and leaf scales.

Many studies have also directly observed the leaf-level uptake of NO_2 (Neubert et al., 1993; Rondon and Granat, 1994; Hereid and Monson, 2001; Sparks et al., 2001; Teklemariam and Sparks, 2006; Pape et al., 2009; Chaparro-Suarez et al., 2011; Breuninger et al., 2013). Isotope labeling experiments investigating the mechanism of NO_2 uptake have demonstrated that atmospheric NO_2 can be absorbed through the stomata of plant leaves, converted to nitrate (NO_3^-) and nitrite (NO_2^-), and eventually assimilated into amino acids (Rogers et al., 1979; Okano and Totsuka, 1986; Nussbaum et al., 1993; Weber et al., 1995; Yoneyame et al., 2003). The mechanism of NO_2 assimilation is diffusion into the stomata followed by dissolution into the aqueous phase and disproportionation to NO_3^- and NO_2^- in the apoplasm (Lee and Schwartz, 1981a, b). NO_2 can also be transformed to nitrate and nitrite through scavenging by antioxidants, most notably ascorbate (Ramge et al., 1993). The influence of ascorbate on foliar uptake was theoretically calculated by Ramge et al. (1993) and experimentally demonstrated by Teklemariam and Sparks (2006). The enzyme nitrate reductase converts NO_3^- to NO_2^- in the cytosol, and NO_2^- is then transported into the plastids where it is further reduced by the enzyme nitrite reductase to ammonium (NH_4^+), the product required for amino acid synthesis (Ammann et al., 1995; Tischner, 2000; Teklemariam and Sparks, 2006). Alternatively, NO_2 can deposit directly onto the leaf cuticles or a leaf-surface water film (Burkhardt and Eiden, 1994). However, foliar uptake of NO_2 has been demonstrated to be controlled primarily by the stomata, with deposition to the leaf surface representing only a small fraction of the total NO_2 flux (Thoene et al., 1991; Gessler et al., 2000; Chaparro-Suarez et al., 2011). Strong correlations have been observed among NO_2 concentrations, stomatal conductances, and the NO_2 deposition flux, suggesting foliar uptake is mainly controlled by stomatal aperture and internal leaf resistances (Johansson, 1987; Thoene et al., 1991; Rondon et al., 1993; Meixner et al., 1997; Chaparro-Suarez et al., 2011; Breuninger et al., 2013).

Despite the large existing body of research on the leaf-level deposition of NO_2 to vegetation, there are still discrepancies present in NO_2 exchange rates and the role of mesophilic processes. Many laboratory experiments have failed to measure uptake rates necessary to describe the observed 20 %–50 % reduction of soil-emitted NO_x (Hanson and Lindberg, 1991; Breuninger et al., 2013), despite the many modeling studies that have suggested dry deposition makes up most of this reduction (Jacob and Wofsy, 1990; Yienger and Levy, 1995; Ganzeveld et al., 2002a; Geddes and Murphy, 2014). Photolysis gradients and reaction of NO_x to form higher nitrogen oxides could account for a large fraction of this reduction in soil NO_x, as has been suggested by Min et al. (2012, 2014), but the relative importance of dry deposition processes versus in-canopy chemical transformations is still a matter of considerable uncertainty (Lerdau et al., 2000; Ganzeveld et al., 2002a). Another controversy is the existence of a compensation point – a concentration below which leaves would instead act as a source of NO_x. Compensation points of 0.1–3.2 ppb NO_2 have been observed in a number of laboratory chamber studies, suggesting trees instead may serve as a large source of NO_x in forests (Johansson, 1987; Rondon et al., 1993; Hereid and Monson, 2001; Sparks et al., 2001; Teklemariam and Sparks, 2006). Emission of NO at these low NO_x mixing ratios has also been detected in laboratory chamber studies (Wildt et al., 1997; Hereid and Monson, 2001). More recent laboratory studies of leaf level deposition have, however, questioned the existence of a compensation point (Chaparro-Suarez et al., 2011; Breuninger et al., 2013). Most observations of NO_x canopy fluxes and atmospheric models predict or assume substantial NO_x deposition at concentrations as low as 0.1 ppb, typical of NO_x mixing ratios in remote areas (Jacob and Wofsy, 1990; Wang and Leuning, 1998; Lerdau et al., 2000; Sparks et al., 2001; Wolfe and Thornton, 2011; Min et al., 2012; Geddes and Murphy, 2014). However, some modeling studies have suggested that an NO_2 compensation point is necessary to describe (Seok et al., 2013) or has only a small effect on canopy fluxes in most regions (Ganzeveld et al., 2002a). More research is thus needed on leaf and canopy-level processes to understand the full complexity of the soil–canopy–atmosphere system.

To understand the leaf-level processes affecting ecosystem-scale atmosphere–biosphere NO_x exchange, we have conducted laboratory experiments measuring NO and NO_2 fluxes to the native California tree species *Quercus agrifolia* (Fig. 1) using a branch enclosure system and direct laser-induced fluorescence (LIF) detection of NO_2 (Fig. 2). With the LIF technique we are able to measure NO_x

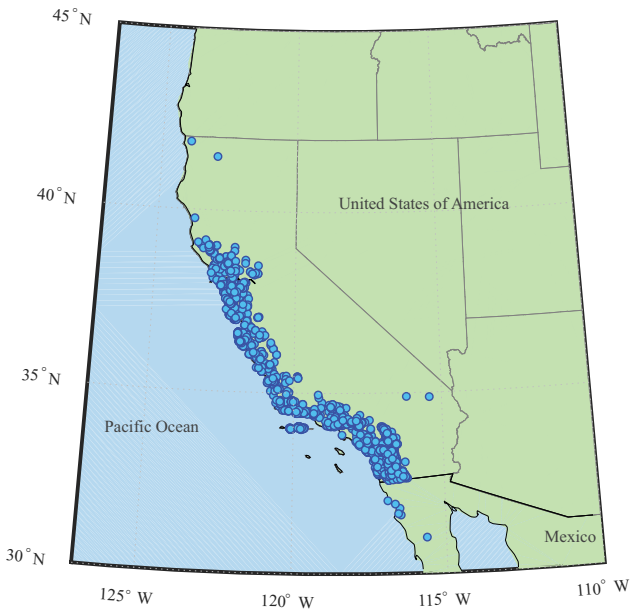

Figure 1. Species distribution map of *Quercus agrifolia*. Each dot represents an observation of *Q. agrifolia* occurrence. Data provided by the participants of the Consortium of California Herbaria.

exchange fluxes with high specificity and sensitivity at trace NO_x mixing ratios relevant to forested environments. We investigated the existence of an NO_2 and NO compensation point and the rate of NO_x foliar uptake under controlled conditions. To our knowledge this is the first leaf-level uptake experiment that has been performed on a North American tree species.

2 Materials and methods

2.1 *Quercus agrifolia* samples

NO_x uptake by *Quercus agrifolia* (coastal live oak) was investigated in the laboratory. Three *Quercus agrifolia* individuals were purchased from a local native California plant nursery (Native Here Nursery), where the plants were grown from seeds and cuttings collected in Contra Costa County. The tree specimens were grown in a nutrient-rich commercial soil mixture (a mixture of orchard potting soil and EB stone cactus mix) at the Jane Grey Research Greenhouse at the University of California, Berkeley. The trees were 2–3 years old when measurements were taken.

2.2 Laser-induced fluorescence detection

NO_2 was measured using LIF. A blue diode laser (Z-Laser ZM18H3) centered at a wavelength of 405 nm was focused into each detection cell and made 20 passes in White multipass optical configuration (Fig. 2b) (Thornton et al., 2000; Fuchs et al., 2009). Upon absorption of a visible photon, NO_2 undergoes a transition from the $^2A_1$ ground to the $^2B_2$ excited electronic state. The excited NO_2 molecule is either quenched by collision or emits a red-shifted photon as it relaxes back to ground state (e.g., Thornton et al., 2000). These emitted photons were detected using a red-sensitive photomultiplier tube (PMT) (Hamamatsu H7421-50). To minimize collisional quenching, each detection cell was maintained at a pressure of around 0.4 kPa. Excitation at 405 nm was chosen because it is near the region of maximum absorption in the NO_2 spectrum and is not subject to interferences from absorption by water vapor or O_3 (Matsumoto and Kajii, 2003).

Calibrations were performed every hour by diluting NO (4.97 ppm ± 5 %, Praxair) and NO_2 standard gases (5.08 ppm ± 5 %, Praxair) to 1–10 ppb in humidified (RH ∼ 60 %) zero air. The limit of detection (LOD) for the detection cells is described as follows:

$$\mathrm{LOD} = \frac{S/N}{m}\sqrt{\frac{2b}{t}}, \quad (1)$$

where m is the slope of the calibration curve constructed from standard dilutions, b is the PMT signal at 0 ppb NO or NO_2, S/N is the desired signal-to-noise ratio, and t is the time of signal averaging. At a S/N of 2 and signal averaging over 5 min, the LOD for detection cells 1–4 was 15, 4, 10, and 30 ppt, respectively. NO_2 in the incoming and outgoing airstreams was measured simultaneously in the first two detection cells. In the second two detection cells, NO was quantitatively converted to NO_2 in the presence of excess ozone, allowing for detection of total NO_x (Fig. 2a). Ozone was produced using an ozone generator (Jelight 600), and flow rates of ozone delivered were adjusted to achieve unity conversion of NO to NO_2.

2.3 Dynamic chamber system

The NO_x flux measurements were performed with a dynamic branch enclosure system, consisting of a thin transparent double-walled Teflon film (FEP) bag (American Durafilm), which transmits 90 % of photosynthetically active radiation. The chamber was illuminated by an LED diode array of 430–475 and 620–670 nm lights (Apollo Horticulture). This light source was selected because it does not emit wavelengths below 420 nm, where NO_2 dissociates, preventing loss of NO_2 to photodissociation and resultant photochemistry. In order to ensure turbulent mixing and minimal aerodynamic and boundary layer resistances, a Teflon-coated fan was installed inside the inner chamber (Meixner et al., 1997; Pape et al., 2009; Breuninger et al., 2013).

Before experiments with *Quercus agrifolia* individuals, the deposition to an empty chamber was measured and background subtracted from subsequent branch measurements. The measured loss of NO_2 to chamber walls was 5 % of the NO_2 mixing ratio flowing into the chamber. This corresponded to a maximum loss of 0.4 ppb at 8 ppb NO_2 and minimum loss of 0.05 ppb at 1 ppb NO_2. Emission of less

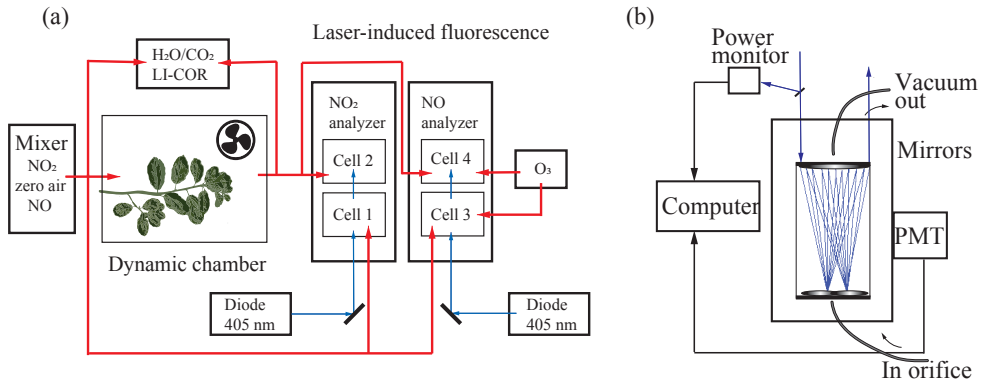

Figure 2. Schematic of the experimental dynamic chamber **(a)** and laser-induced fluorescence detection **(b)** setups.

than 0.05 ppb NO_2 from the Teflon walls was also observed when chamber lights were turned on with 0 ppb NO_2 flowing through the system. It is likely that the chamber walls buffer uptake of NO_2, but this is a minor effect, as the wall emission observed was a tiny fraction of the measured fluxes.

During measurements, the enclosed branch was exposed to known amounts of either NO_2 or NO mixed with zero air. The inner chamber had an inner diameter of 20 cm, a length of 40 cm, and a total volume of 13 L (American Durafilm 200A Teflon FEP). Flow rates into the inner chamber (Q) during experiments were typically 5 L min^{-1}, creating a residence time in the chamber of 3 min. The outer chamber had an inner diameter of 30 cm and a length of 55 cm (American Durafilm 500C20 Teflon FEP). Zero air at a flow rate of 3 L min^{-1} constantly fumigated the outer bag, serving as a buffer region to ensure the laboratory air, with high mixing ratios of NO_x, did not diffuse into the bag enclosing the branch.

The photosynthetic photon flux density (PPFD) was monitored outside the chamber with a LiCor quantum sensor (LiCor LI-190SA). The flux density measured above the chamber was 1190 µmol m^{-2} s^{-1}, approximately the PPFD for Berkeley, California, at noon during the month of October. This is well above the photon flux required to achieve maximal stomatal aperture for broadleaf evergreen trees (von Caemmerer and Farquhar, 1981; Chaparro-Suarez et al., 2011; Breuninger et al., 2013). We confirmed this assumption by covering the lights with a filter to reduce the intensity by 40 % and monitoring CO_2 and H_2O exchange. No reduction in the exchange rates of these gases were observed. The relative humidity of air entering the chamber was maintained at 50 %–65 % in all experiments by flowing zero air through a bubbler before mixing with NO_x. Measurements of NO_x exchange fluxes occurred under a light/dark cycle with a photoperiod of 12 h and a temperature of 26/22±2 °C. No change in NO_x uptake was observed when heating the chamber with the lights off or cooling the chamber with the lights on. We therefore expect no significant temperature effects caused by the 4 °C difference in temperature between light and dark periods. We also observed a relative humidity increase in the delivered air of about 2 % with the lights off, but do not expect this increase to produce any significant changes in NO_x deposition or plant physiology (von Caemmerer and Farquhar, 1981; Chaparro-Suarez et al., 2011).

Exchange of CO_2 and H_2O with the leaves were monitored with a LiCor-6262 H_2O/CO_2 analyzer operating in differential mode. Flows of 0.1 L min^{-1} of air entering and exiting the chamber were diverted to the LiCor analyzer to measure the CO_2 assimilation and transpiration rates. To measure the CO_2 content and relative humidity of air delivered to the chamber, 0.5 L min^{-1} of the humidified zero air / NO_x mixture was diverted to a second external 1.5 L cuvette. The temperature and relative humidity of air entering the chamber were measured with a temperature and relative humidity module in the external cuvette (TE Connectivity HTM2500LF). The CO_2 mixing ratios in the external chamber were monitored with a Vaisala CarboCap GMP343 sensor.

2.4 NO_x flux densities

The leaf-level exchange flux of NO or NO_2 (F_{NO_x}) was calculated according to Eq. (2):

$$F_{NO_x} = \frac{Q \cdot (C_0 - C_i)}{A}, \quad (2)$$

where Q is the flow rate (m^3 s^{-1}), A is the enclosed leaf area (m^2), C_0 is the concentration leaving the chamber, and C_i is the concentration entering the chamber (nmol m^{-3}). The calculated flux is related to a deposition velocity (Vd_{NO_x}) by Eq. (3):

$$F_{NO_x} = -Vd_{NO_x} \cdot (C_0 + C_{comp}), \quad (3)$$

where C_{comp} is the compensation point, the concentration of NO_2 below which the tree would instead act as a source of NO_x. The deposition velocities were calculated through weighted least-square regression of calculated fluxes and outlet NO_x concentrations (C_o). The absolute value of the slope

of the regression line was equal to the deposition velocity, with the x intercept representing the compensation point concentration. The precision error in the NO_x exchange flux (σ_F) was calculated through propagation of the error in the inlet (σ_{C_i}) and outlet (σ_{C_o}) concentrations (Eq. 4).

$$\sigma_F = \frac{Q}{A}\sqrt{\sigma_{C_i}^2 + \sigma_{C_o}^2} \quad (4)$$

σ_{C_i} and σ_{C_o} were estimated as the larger of the error in the calibration slopes and the standard deviation of the 5 min signal average. From observations in daily deviations of the flow rate and error in measured leaf area using the ImageJ software (Schneider et al., 2012), we estimate the error in $\frac{Q}{A}$ to be a maximum of 0.005 cm s^{-1}. This usually was only a minor contribution to the total error in the NO_x exchange flux.

The calculated deposition velocity was used to find the total resistance to deposition, R, via Eq. (5).

$$Vd_{NO_x} = \frac{1}{R} \quad (5)$$

The total resistance is described by the canopy stomatal resistance model (Baldocchi et al., 1987) and defined in Eqs. (6)–(7).

$$R = R_a + R_b + R_{leaf}, \quad (6)$$

$$R_{leaf} = \left(\frac{1}{R_{cut}} + \frac{1}{R_{st} + R_m}\right)^{-1}, \quad (7)$$

where R_{leaf} is the total leaf resistance and R_a, R_b, R_{cut}, R_{st}, and R_m are the aerodynamic, boundary layer, cuticular, stomatal, and mesophilic resistances, respectively. The aerodynamic resistance is characterized by the micrometeorology above a surface and is dependent upon the wind speed and turbulence of air flow. The boundary layer resistance describes the diffusion of a molecule through a shallow boundary of air above a surface and is dependent on microscopic surface properties, diffusivity of the gas species, wind speed, and turbulence of air flow (Baldocchi et al., 1987). R_{cut}, R_{st}, and R_m are the resistances associated with deposition to the leaf cuticles or through the stomata, and are dependent upon plant physiology.

The chamber fan, installed to create turbulent mixing, allowed for the assumption that R_a was negligible (Pape et al., 2009; Breuninger et al., 2012). R_b is chamber-specific, and has typically not been measured in previous chamber experiments of NO_2 leaf-level deposition (Chaparro-Suarez et al., 2011; Breuninger et al., 2012, 2013). R_b was experimentally measured in this study by placing a tray of activated carbon into the chamber (assumed to have zero surface resistance to deposition of NO_2) and calculating the deposition flux of NO_2. The leaf components to the total deposition resistance were determined through dark and light experiments. During dark experiments, the stomata were closed (confirmed with measurements of CO_2 and H_2O exchange), and the deposition observed was assumed to be entirely driven by deposition to the cuticles.

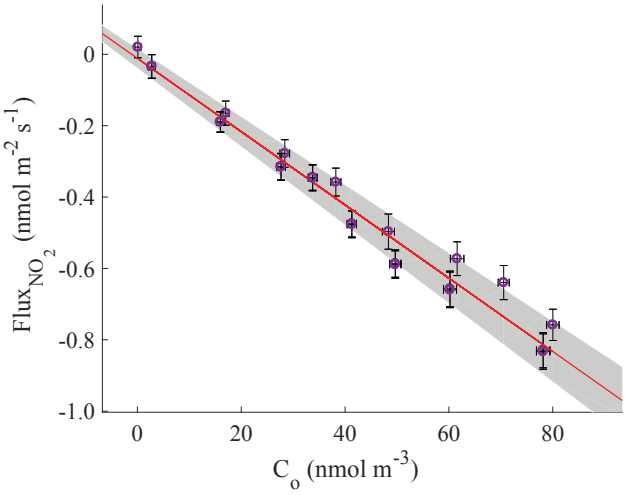

Figure 3. Flux to a 5.1 cm diameter dish filled with activated charcoal. The chemical surface resistance to deposition is approximately zero, so the deposition velocity for deposition of NO_2 to the surface of the charcoal dish is the reciprocal of the boundary layer resistance. The line of best fit is $(0.51 \pm 0.032)\, C_o$, where C_o is the concentration of NO_2 in the outgoing airstream.

3 Results

3.1 Determination of the boundary resistance R_b

To estimate the chamber boundary layer resistance and test the assumption that $R_b \ll R_{leaf}$, a dish of activated carbon, which theoretically has zero chemical resistance to deposition of NO_2, was placed inside the chamber. The boundary layer resistance was considered to be the only component of the total resistance to deposition. The deposition velocity of NO_2 to activated carbon was measured as 0.52 ± 0.06 cm s^{-1}, corresponding to a boundary layer resistance to NO_2 deposition of 1.94 ± 0.02 s cm^{-1} (Fig. 3). This boundary resistance is approximately double what was measured by Pape et al. (2009) – a reasonable difference given differences in chamber design (Fig. 2). The R_b for NO_2 was scaled with the ratio of diffusivities of NO_2 and NO in air to obtain the resistance to deposition of NO of 2.59 ± 0.03 s cm^{-1}. However, with a branch enclosed inside the chamber, the effective boundary resistance to deposition will likely be reduced, as the surface roughness and surface area for deposition is increased (Galbally and Roy, 1980; Pape et al., 2009). The boundary resistances presented above thus serve as an upper limit for R_b with vegetation inside the chamber.

The boundary resistance was also estimated in an additional experiment (not shown) in which a de-ionized water-soaked Whatman no. 1 filter paper was placed inside the chamber and the evaporation of water vapor into the chamber filled with dry zero air was measured. The emission flux of water vapor from the filter paper was calculated in a similar manner to that of NO_x deposition flux (Eq. 2). The conductance to water vapor was then calculated via

$$\frac{Q \cdot \left(P_{H_2O}\right)}{A} = g_w(P_{sat} - P_{H_2O}), \quad (8)$$

where P_{H_2O} is the partial pressure of water vapor inside the chamber, P_{sat} is the saturation vapor pressure at the temperature in the chamber, and g_w is the conductance to water vapor. The measured conductance to water vapor was scaled with the ratio of diffusivities of NO_2 to water vapor (D_{NO_2}/D_{H_2O}) and inverted to find the NO_2 boundary layer resistance:

$$R_b = \frac{D_{H_2O}}{D_{NO_2}} \frac{1}{g_w}. \quad (9)$$

The boundary resistance to NO_2 deposition by this method was found to be $2\,s\,cm^{-1}$, essentially identical to the measurement on the activated-carbon.

3.2 NO_x deposition velocity and compensation point concentration

The deposition velocities and compensation points were respectively calculated as the slope and x-axis intercept of the regression line between NO_x exchange flux and chamber NO_x concentrations (Fig. 4). The detection limit was the dominant source of error in the estimation of the NO exchange flux and compensation point. The large relative uncertainties in NO flux measurements were caused by the much slower deposition of NO compared with that of NO_2, inhibiting our ability to observe the very small changes between the NO concentration in the chamber and the incoming airstream (Fig. 4). Additional uncertainty in NO_2 flux measurements because of enhanced water vapor quenching of excited-state NO_2 should be minimal, as calibrations and measurements were performed at equivalent relative humidities. However, transpiration of the enclosed leaves caused the absolute humidity within chamber to be enhanced by 0.3 %–0.5 % relative to the incoming airstream. We expect this to result in a maximum error in calculated NO_2 mixing ratios of 1 %–1.75 % (Thornton et al., 2000), resulting in maximum errors in the calculated fluxes and deposition velocities of 2 % and 4 %, respectively. This 4 % error in the calculated deposition velocity during lights-on experiments is less that the uncertainty of the linear fit (Fig. 4).

Correlation coefficients, deposition velocities, compensation points, and statistical testing of the compensation point for NO_2 and NO deposition are shown in Table 1 and Table 2, respectively, and were calculated according to Breuninger et al. (2013). For NO_2 experiments, only one dark and one light experiment with *Quercus agrifolia* 1 were found to have statistically significant ($\alpha = 0.05$) nonzero intersections with the x axis (Table 1). The range of C_{comp} measured was −0.02 to 0.300 ppb NO_2, with probabilities of $C_{comp} = 0$ ranging from 10.3 % to 91.6 % (excluding the two *Quercus agrifolia* 1 experiments) (Table 1). Conversely, all three *Quercus agrifolia* individuals during all dark and light NO deposition experiments demonstrated compensation points significantly above zero, ranging from 0.74 to 3.8 ppb NO. The average compensation point was calculated as 0.84 ± 0.32 ppb NO during light experiments and 2.4 ± 1.1 ppb NO during dark experiments (Table 2).

Student's t tests (not shown) demonstrated that deposition velocities and compensation points measured during NO

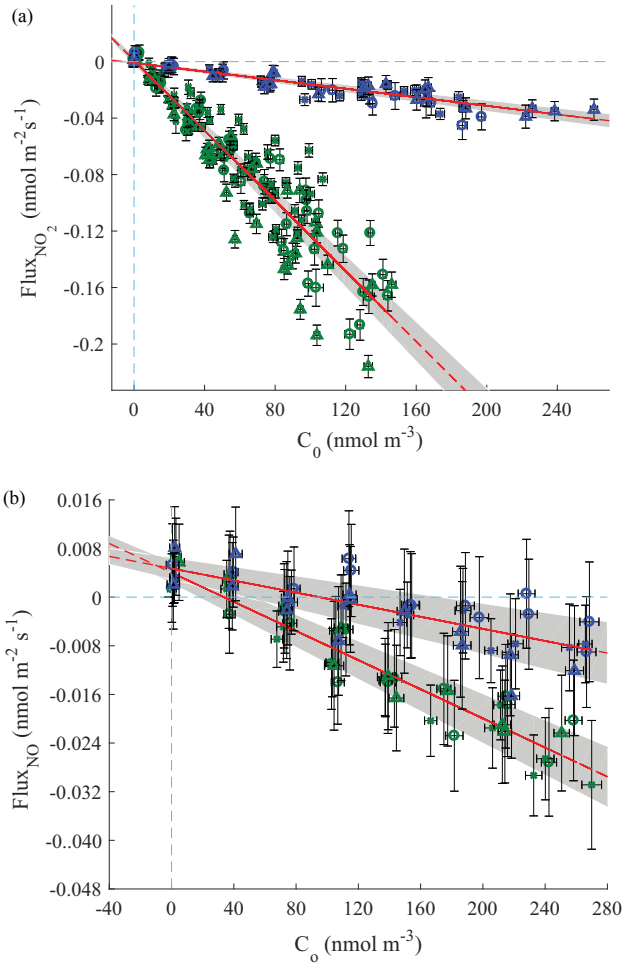

Figure 4. NO_2 **(a)** and NO **(b)** fluxes versus the outlet concentrations for all *Quercus agrifolia* individuals with the chamber lights on (green) and off (blue). The line of best fit is shown in red and was calculated to minimize the weighted residuals in both the x and y axes. The blue dotted lines show where flux and C_o are zero. A significantly positive ($\alpha = 0.5$) x intercept occurs for NO, but not NO_2 experiments.

Table 1. Parameters of NO_2 bivariate linear least-square fitting regression analysis.

Run	N	R^2	$[NO_2]_{comp}$ (ppb)	$P([NO_2]_{comp} = 0)$ (%)	V_{dep} ($cm\,s^{-1}$)
Q. agrifolia 1, light					
1	13	0.979	0.056 ± 0.013	42.7	0.10 ± 0.013
2	13	0.950	0.046 ± 0.19	63.7	0.12 ± 0.023
3	16	0.978	0.099 ± 0.086	3.87	0.15 ± 0.016
4	16	0.958	0.077 ± 0.14	28.7	0.12 ± 0.021
All	58	0.927	0.080 ± 0.10	11.6	0.12 ± 0.012
Q. agrifolia 2, light					
1	16	0.963	0.10 ± 0.12	10.3	0.08 ± 0.011
2	5	0.969	-0.01 ± 0.96	83.8	0.12 ± 0.014
3	9	0.997	0.023 ± 0.032	20.3	0.16 ± 0.011
4	16	0.974	-0.019 ± 0.074	61.9	0.14 ± 0.017
5	15	0.979	0.015 ± 0.082	72.7	0.12 ± 0.014
All	61	0.845	-0.0077 ± 0.091	91.6	0.11 ± 0.014
Q. agrifolia 3, light					
1	11	0.969	0.016 ± 0.18	87.4	0.12 ± 0.024
2	15	0.961	0.074 ± 0.16	39.1	0.18 ± 0.029
3	5	0.990	0.30 ± 0.20	5.9	0.12 ± 0.038
All	31	0.830	0.019 ± 0.064	77.6	0.14 ± 0.029
All *Q. agrifolia*, light	150	0.885	0.030 ± 0.072	41.3	0.123 ± 0.0092
Q. agrifolia 1, dark					
1	16	0.964	0.056 ± 0.14	0.9*	0.022 ± 0.0034
Q. agrifolia 2, dark					
1	16	0.858	-0.16 ± 0.47	50.8	0.016 ± 0.0050
2	12	0.932	-0.34 ± 0.40	11.8	0.013 ± 0.0038
All	28	0.853	-0.24 ± 0.32	15.6	0.015 ± 0.0030
Q. agrifolia 3, dark					
1	14	0.900	-0.30 ± 0.48	24.1	0.015 ± 0.0042
2	11	0.909	-0.001 ± 0.69	36.7	0.015 ± 0.0057
All	25	0.898	-0.22 ± 0.38	25.3	0.014 ± 0.0029
All *Q. agrifolia*, dark	69	0.881	-0.16 ± 0.24	12.2	0.015 ± 0.0018

* Significant nonzero compensation point.

and NO_2 lights-on and lights-off experiments were not significantly different (to the $\alpha = 0.05$ confidence level) between different *Quercus agrifolia* individuals. Deposition velocities for NO_2 light experiments were between 0.08 and $0.18\,cm\,s^{-1}$, with a deposition of $0.123 \pm 0.009\,cm\,s^{-1}$ calculated from the regression of all light experiments. Dark experiments resulted in deposition velocities between 0.013 and $0.022\,cm\,s^{-1}$, with a deposition velocity of $0.015 \pm 0.001\,cm\,s^{-1}$ calculated from the regression of all dark experiments (Table 1). NO demonstrated much slower deposition, with deposition velocities from all light and dark experiments calculated as 0.012 ± 0.002 and $0.005 \pm 0.002\,cm\,s^{-1}$, respectively (Table 2). Despite the large compensation point measured for NO, the leaf emission fluxes of NO were a maximum of only $8\,pmol\,m^{-2}\,s^{-1}$ at 0.1 ppb NO, approximately half of the deposition flux measured for NO_2 at 0.1 ppb (Fig. 4). At typical NO_2/NO ratios and gradients measured in forest canopies, the leaf-level NO_2 and NO exchange fluxes measured make dry stomatal deposition to *Quercus agrifolia* a net sink of NO_x within the canopy.

3.3 Resistances to leaf-level NO_x deposition

The deposition velocity measured from linear regression of NO_x exchange fluxes and NO_x chamber concentrations is the

Table 2. Parameters of NO bivariate linear least-square fitting regression analysis.

Run	N	R^2	$[NO_2]_{comp}$ (ppb)	$P([NO_2]_{comp} = 0)$	V_{dep}
Q. agrifolia 1					
Light	17	0.874	0.74 ± 0.65	3.5*	0.011 ± 0.0032
Dark	13	0.699	3.8 ± 2.2	0.52*	0.0040 ± 0.0025
Q. agrifolia 1					
Light	14	0.954	0.76 ± 0.49	0.92*	0.013 ± 0.0027
Dark	10	0.866	1.7 ± 1.0	1.1*	0.0046 ± 0.0018
Q. agrifolia 1					
Light	12	0.936	1.3 ± 0.60	0.17*	0.0123 ± 0.0029
Dark	15	0.803	2.0 ± 1.0	2.5*	0.0074 ± 0.0033
All *Q. agrifolia*					
Light	13	0.908	0.84 ± 0.32	< 0.01*	0.012 ± 0.0015
Dark	13	0.602	2.4 ± 1.1	< 0.01*	0.0050 ± 0.0016

* Significant nonzero compensation point.

inverse of the total resistance to deposition (Eq. 6), with R_a assumed to be zero. The total resistance in the chamber is thus

$$R = R_b + \left(\frac{1}{R_{cut}} + \frac{1}{R_s^*}\right)^{-1}, \quad (10)$$

where R_s^* is the sum of R_m and R_{st}. The leaf resistance to deposition can then be found by subtracting the boundary layer resistance from the total resistance. Total leaf resistances, R_{leaf}, were calculated using the boundary layer resistances for NO_2 and NO of 1.94 ± 0.02 and 2.59 ± 0.03 s cm^{-1}, respectively. During the dark experiments, R_{leaf} is equal to R_{cut}, and the deposition velocity measured was estimated as the inverse of the sum of the boundary and cuticular resistances. After calculation of R_{cut} from dark experiments, the sum of the stomatal and mesophilic contributions (R_s^*) to the total leaf resistance was determined. R_b, R_{cut}, and R_s^* are shown in Table 3. It should be noted that since the reported R_b is the maximum possible boundary resistance, the reported R_{cut} and R_s^* are lower limits. If we were to assume the chamber boundary resistance with the branch enclosed is insignificant (~ 0 s cm^{-1}), this would introduce maximum systematic 30 % and 3 % errors to the calculated NO_2, R_s^* and R_{cut}, respectively (giving an R_s^* of 9.2 ± 0.9 s cm^{-1} and an R_{cut} of 67 ± 8 s cm^{-1}). The errors in the calculated NO resistances would be negligible.

It is possible that the stomata were not entirely closed during dark experiments. Evidence exists that nocturnal stomatal conductance can be large enough to allow for transpiration (Dawson et al., 2007), and low (within the range of uncertainty observed for the LICOR-6262) emission of water vapor during dark experiments was measured. However, even if all the deposition during dark experiments was stomatal, this would cause only a 0.5 s cm^{-1} reduction in the calculated R_s^* for NO_2 – less than the uncertainty from the error in the measured deposition velocity (~ 10 % error). The cuticular resistances reported here during dark experiments are nonetheless atmospherically relevant to nighttime NO_x deposition.

Table 3. Summary of deposition resistance parameters of *Quercus agrifolia*.

Gas	R_b (s cm^{-1})	R_{cut} (s cm^{-1})	R_s^* (s cm^{-1})
NO_2	1.94 ± 0.02	65 ± 8	6.9 ± 0.9
NO	2.59 ± 0.03	200 ± 60	140 ± 40

4 Discussion

4.1 NO_x deposition velocities and compensation points

The strong linear dependence between NO_2 fluxes and NO_2 chamber concentrations that we observe is consistent with previous observations that NO_2 exchange is largely driven by NO_2 concentration differences between the atmosphere and gaseous phase of the leaf (Rondon and Granat, 1994; Gessler et al., 2000; Hereid and Monson, 2001; Sparks et al., 2001; Teklemariam and Sparks, 2006; Pape et al., 2009; Chaparro-Suarez et al., 2011; Breuninger et al., 2012). Our measurements of NO_2 stomatal resistance parameters for *Quercus agrifolia* represent a stomatal deposition velocity ($1/R_s^*$) of 0.14 ± 0.02 cm s^{-1}. This value is similar to the range of 0.1–

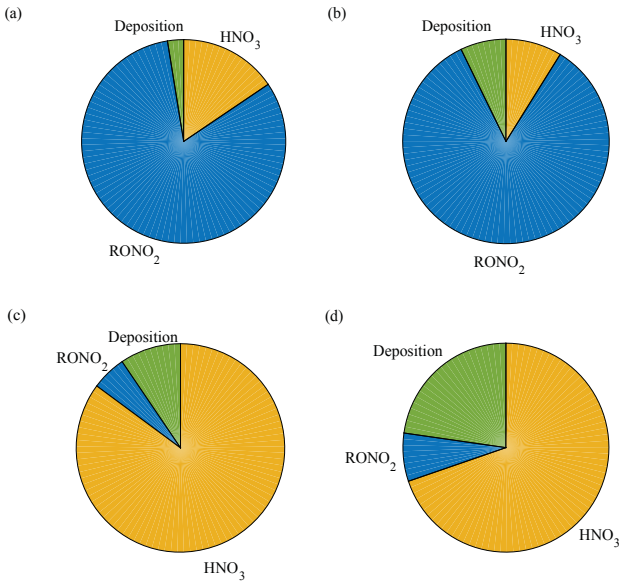

Figure 5. Model predictions of the fraction of NO_x loss to alkyl nitrate formation, nitric acid formation, and deposition in a *Q. agrifolia* woodland. The model was run using scenarios with only soil emissions and LAI of 1 m^2 m^{-2} **(a)**, only soil emissions and LAI of 3 m^2 m^{-2} **(b)**, $C_{NO_x(adv)} = 10$ ppb and LAI of 1 m^2 m^{-2} **(c)**, and $C_{NO_x(adv)} = 10$ ppb and LAI of 3 m^2 m^{-2} **(d)**.

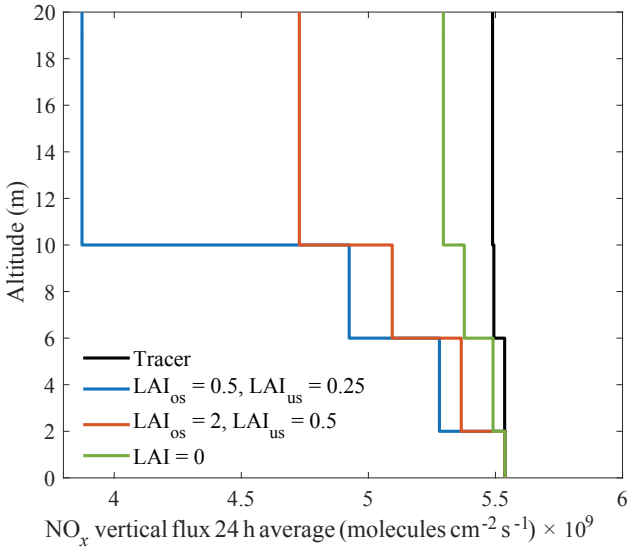

Figure 6. 24 h average vertical fluxes of NO_x predicted by the 1-D multibox model for a California oak woodland using the leaf resistances measured in this study. Model runs were conducted for low (red) and high (blue) LAI cases and for a no-deposition scenario (green).

0.15 cm s^{-1} that Chapparo-Suarez et al. (2011) found for two European oak tree species, *Quercus robur* and *Quercus ilex*. The deposition velocity measured here for *Quercus agrifolia* is also much larger than 0.007–0.042 cm s^{-1} range found for Norway spruce (*Picea abies)* by Breuninger et al. (2012), but surprisingly comparable, given the differences in plant species, to the 0.12 cm s^{-1} deposition velocity found for maize (*Zea mays*) by Hereid and Monson (2001). We also find here an NO_2 flux at 5 ppb of 0.2 nmol m^{-1} s^{-1}, similar in magnitude to the 0.1, 0.15–1.5, and 0.18 nmol m^{-1} s^{-1} fluxes measured for *Fagus sylvatica* (Gessler et al., 2000), tropical Panamanian native trees (Sparks et al., 2001), and periwinkle (*Catharanthus roseus)* (Teklemariam and Sparks, 2006), respectively.

Resistance parameters reported above for NO deposition to *Quercus agrifolia* represent a stomatal deposition velocity of 0.007 ± 0.002 cm s^{-1} and cuticular deposition velocity of 0.005 ± 0.001 cm s^{-1}. This observation of very minor NO uptake – at least an order of magnitude less than that of NO_2 uptake – is also consistent with previous observations (Hanson and Lindberg, 1991; Hereid and Monson, 2001; Teklemariam and Sparks, 2006). We also detected a statistically significant NO compensation point, with low emissions up to 8 pmol m^{-2} s^{-1} observed below 1 ppb. These observations are similar to the 8–14 pmol m^{-2} s^{-1} emission fluxes of NO reported by Hereid and Monson (2001) and Teklemariam and Sparks (2006) at low NO_x concentrations.

No significant NO_2 compensation point was found for our measurements of *Quercus agrifolia* NO_x uptake. Many previous studies have reported NO_2 compensation points, ranging from 0.1 to 3.0 ppb, implicating trees as a constant source of NO_x in forest ecosystems (Gessler et al., 2000; Hereid and Monson, 2001; Sparks et al., 2001; Teklemariam and Sparks, 2006). Our findings of a lack of NO_2 compensation point support field observations and modeling studies that have recognized NO_2 dry deposition to vegetation as an important NO_x loss process in forests (Jacob and Wofsy, 1990; Ganzeveld et al., 2002b; Geddes and Murphy, 2014). Our results also support the works of Chaparro-Suarez et al. (2011) and Breuninger et al. (2013), who did not find evidence of an NO_2 compensation point.

The primary difference in our experimental setup, compared to previous dynamic chamber studies that have found an NO_2 compensation point, is the use of a direct NO_2 measurement technique. Measurements of a significant NO_2 compensation point have mostly been obtained using techniques requiring conversion of NO_2, followed by chemiluminescence detection of NO (Gessler et al., 2000; Hereid and Monson, 2001; Sparks et al., 2001; Teklemariam and Sparks, 2006). Such methods have utilized either nonspecific photolytic (Gessler et al., 2000; Hereid and Monson, 2001), luminol (Sparks et al., 2001), or catalytic conversion (Teklemariam and Sparks, 2006) techniques, which may have also resulted in the conversion of PAN, HONO, HNO_3, and other organic nitrates, as well as interferences from alkene + ozone reactions (Carter et al., 2005; Reed et al., 2016). If any of these interfering compounds are not excluded from the cham-

ber system, outgas from the chamber itself, or form from reactions of biogenic emissions, this would cause an enhancement in the observed NO_2 compensation point, and a suppression of observed deposition velocity. Our measurements of NO_2 mixing ratios also demonstrate a much higher degree of precision, due largely to a lower detection limit, than comparable experiments with specific photolytic conversion and chemiluminescence measurement of NO_2 (Chaparro-Suarez et al., 2011; Breuninger et al., 2012, 2013). Additionally, previous chamber measurements have sometimes employed chamber setups that would let in a substantial amount of UV light, yet did not exclude photochemical reactions between NO_2, NO, and O_3. Such corrections are excluded here because of our use of chamber lights with only wavelengths above 420 nm. To avoid this issue, other experiments have instead involved a setup including a simultaneously measured blank chamber, which would theoretically allow for correction for any reactions resulting from photolysis of NO_2, O_2, or O_3 (Gessler et al., 2000; Hereid and Monson, 2001). Such corrections might be complicated by secondary chemistry not present in our experiments.

4.2 Implication for canopy NO_x loss

Resistance parameters reported above (Table 3) were used in a 1-D seven-layer multibox model representing chemical reactions, vertical transport, and leaf-level processes scaled to the canopy level to assess the impacts of NO_x deposition velocities on the NO_x lifetime and fluxes. The model is constructed in a manner similar to Wolfe and Thornton (2011) with the following modifications: the model domain consists of seven well-mixed vertical layers extending to a planetary boundary layer height of 1000 m, with the forest canopy represented by the first three layers; NO_x cuticular and stomatal resistances are adjustable input parameters; and the chemistry implemented in the model is the simplified reaction mechanism presented in Brown and Cohen (2012). The 1-D model was run for meteorological conditions representing the native habitat of *Quercus agrifolia* and two different leaf area indices (LAIs), approximately representing the lower and upper limits of LAIs found in California oak woodlands. As shown in Fig. 5a and b, the model predicts NO_x deposition to *Q. agrifolia* accounts for 3 %–7 % of the total NO_x loss within the boundary layer if the only source of NO_x is emissions from the soil. This represents a total NO_x lifetime of 7–7.5 h in the boundary layer, and a lifetime to deposition of 4–11 days in the boundary layer and 0.5–1.2 h below the canopy. Under these scenarios approximately 15–30 % of soil-emitted NO_x is removed in the canopy (Fig. 6) – on the lower end of the range of 25 %–80 % reduction observed in field studies (Jacob and Wofsy, 1990; Lerdau et al., 2000; Ganzeveld et al., 2002a; Min et al., 2014).

The coastal regions of California where *Q. agrifolia* is found frequently experience much higher NO_x mixing ratios of 10–50 ppb. This is particularly important for oak woodlands of the San Francisco Bay and Los Angeles areas, where anthropogenic emissions from nearby urban centers are the majority of the NO_x source. To account for this extra NO_x source, additional model runs were performed with an added term accounting for NO_x advection from a more concentrated upwind source ($C_{NO_x(adv)}$), with advection treated as a simple mixing process:

$$\left(\frac{dC_{NO_x}}{dt}\right) = -k_{mix}\left(C_{NO_x} - C_{NO_x(adv)}\right), \quad (11)$$

where $k_{mix} = 0.3\,h^{-1}$ and $C_{NO_x(adv)}$ is 10 ppb.

In this case, deposition to *Q. agrifolia* could account for 10–22 % of the total NO_x loss in the boundary layer (Fig. 5c, d), representing a lifetime to deposition of 5–14 days in the boundary layer and a total NO_x lifetime of 28–33 h. Deposition in this higher NO_x scenario decreased the total NO_x lifetime by 3–8 h, compared with a no-deposition case.

5 Conclusions

This work constitutes the first measurements of NO_2 and NO foliar deposition resistance parameters for a North American tree species. We report observations of leaf-level resistances to NO_2 and NO deposition, corresponding to total deposition velocities of NO_2 and NO of 0.123 ± 0.007 and $0.012 \pm 0.002\,cm\,s^{-1}$ in the light and 0.015 ± 0.001 and $0.005 \pm 0.002\,cm\,s^{-1}$ in the dark, respectively. No compensation point was observed for NO_2, but compensation points of 0.74–3.8 ppb were recorded for NO. The magnitude of NO emission below the compensation point was significantly less than the magnitude of NO_2 uptake in the same concentration range, making *Q. agrifolia* an overall large net sink of NO_x. The observed deposition is large enough to explain canopy reduction factors observed in canopy-level studies, but is at the lower end of estimated global CRFs. The results of the 1-D multibox model demonstrate that the deposition observed accounts for 5 %–20 % of NO_x removal with a NO_x lifetime to deposition of 0.5–1.2 h beneath the canopy of a California oak woodland. We show that foliar deposition of NO_x represents a significant removal mechanism of NO_x and can have a large impact on NO_x mixing ratios and fluxes in such ecosystems. Further investigations of NO_2 deposition to a larger variety of plant species under a range of environmental conditions are needed to accurately understand the global impacts of NO_2 deposition across diverse ecosystems.

Data availability. The data collected in this study can be obtained from the authors upon request. The details and implications of the 1-D multi-box model presented in this publication are being prepared for discussion in an additional paper. Questions relating to this model can be addressed to the authors.

Author contributions. ERD and JC carried out the experiments. ERD performed the data analysis, constructed the 1-D multi-box model, and prepared all figures. MV conceived of the original project idea and constructed the dynamic chamber and laser-induced fluorescence instrument. Modifications to the initial setup were made by ERD. ERD wrote the paper in consultation with RCC. RCC supervised the project.

Competing interests. The authors declare that they have no conflict of interest.

Acknowledgements. We would like to thank the two reviewers for their constructive comments. We also wish to gratefully acknowledge financial support from the National Science Foundation (NSF, AGS-1352972). Additional support was provided by an NSF Graduate Research Fellowship to Erin R. Delaria.

Edited by: Alex B. Guenther
Reviewed by: Laurens Ganzeveld and one anonymous referee

References

Ammann, M., Vonballmoos, P., Stalder, M., Suter, M., and Brunold, C.: Uptake and assimilation of atmospheric NO_2-N by spruce needles (Picea abies): A field study, Water Air Soil Poll., 85, 1497–1502, https://doi.org/10.1007/Bf00477193, 1995.

Baldocchi, D. D., Hicks, B. B., and Camara, P.: A Canopy Stomatal-Resistance Model for Gaseous Deposition to Vegetated Surfaces, Atmos. Environ., 21, 91–101, https://doi.org/10.1016/0004-6981(87)90274-5, 1987.

Breuninger, C., Oswald, R., Kesselmeier, J., and Meixner, F. X.: The dynamic chamber method: trace gas exchange fluxes (NO, NO_2, O_3) between plants and the atmosphere in the laboratory and in the field, Atmos. Meas. Tech., 5, 955–989, https://doi.org/10.5194/amt-5-955-2012, 2012.

Breuninger, C., Meixner, F. X., and Kesselmeier, J.: Field investigations of nitrogen dioxide (NO_2) exchange between plants and the atmosphere, Atmos. Chem. Phys., 13, 773–790, https://doi.org/10.5194/acp-13-773-2013, 2013.

Browne, E. C. and Cohen, R. C.: Effects of biogenic nitrate chemistry on the NOx lifetime in remote continental regions, Atmos. Chem. Phys., 12, 11917–11932, https://doi.org/10.5194/acp-12-11917-2012, 2012.

Burkhardt, J. and Eiden, R.: Thin Water Films on Coniferous Needles, Atmos. Environ., 28, 2001–2011, https://doi.org/10.1016/1352-2310(94)90469-3, 1994.

Caranto, J. D. and Lancaster, K. M.: Nitric oxide is an obligate bacterial nitrification intermediate produced by hydroxylamine oxidoreductase, P. Natl. Acad. Sci. USA, 114, 8217–8222, https://doi.org/10.1073/pnas.1704504114, 2017.

Carter, W. P. L., Cocker, D. R., Fitz, D. R., Malkina, I. L., Bumiller, K., Sauer, C. G., Pisano, J. T., Bufalino, C., and Song, C.: A new environmental chamber for evaluation of gas-phase chemical mechanisms and secondary aerosol formation, Atmos. Environ., 39, 7768–7788, https://doi.org/10.1016/j.atmosenv.2005.08.040, 2005.

Chaparro-Suarez, I. G., Meixner, F. X., and Kesselmeier, J.: Nitrogen dioxide (NO2) uptake by vegetation controlled by atmospheric concentrations and plant stomatal aperture, Atmos. Environ., 45, 5742–5750, https://doi.org/10.1016/j.atmosenv.2011.07.021, 2011.

Crutzen, P. J.: Role of NO and NO_2 in the Chemistry of the Troposphere and Stratosphere, Annu. Rev. Earth Pl. Sc., 7, 443–472, https://doi.org/10.1146/annurev.ea.07.050179.002303, 1979.

Dawson, T. E., Burgess, S. S. O., Tu, K. P., Oliveira, R. S., Santiago, L. S., Fisher, J. B., Simonin, K. A., and Ambrose, A. R.: Nighttime transpiration in woody plants from contrasting ecosystems, Tree Physiol., 27, 561–575, https://doi.org/10.1093/treephys/27.4.561, 2007.

Fuchs, H., Dube, W. P., Lerner, B. M., Wagner, N. L., Williams, E. J., and Brown, S. S.: A Sensitive and Versatile Detector for Atmospheric NO_2 and NO_x Based on Blue Diode Laser Cavity Ring-Down Spectroscopy, Environ. Sci. Technol., 43, 7831–7836, https://doi.org/10.1021/es902067h, 2009.

Galbally, I. E. and Roy, C. R.: Destruction of Ozone at the Earths Surface, Q. J. Roy. Meteor. Soc., 106, 599–620, https://doi.org/10.1002/qj.49710644915, 1980.

Ganzeveld, L. N., Lelieveld, J., Dentener, F. J., Krol, M. C., Bouwman, A. J., and Roelofs, G. J.: Global soil-biogenic NOx emissions and the role of canopy processes, J. Geophys. Res.-Atmos., 107, 4298, https://doi.org/10.1029/2001jd001289, 2002a.

Ganzeveld, L. N., Lelieveld, J., Dentener, F. J., Krol, M. C., and Roelofs, G. J.: Atmosphere-biosphere trace gas exchanges simulated with a single-column model, J. Geophys. Res.-Atmos., 107, 4297, https://doi.org/10.1029/2001jd000684, 2002b.

Geddes, J. A. and Murphy, J. G.: Observations of reactive nitrogen oxide fluxes by eddy covariance above two midlatitude North American mixed hardwood forests, Atmos. Chem. Phys., 14, 2939–2957, https://doi.org/10.5194/acp-14-2939-2014, 2014.

Gessler, A., Rienks, M., and Rennenberg, H.: NH_3 and NO_2 fluxes between beech trees and the atmosphere – correlation with climatic and physiological parameters, New. Phytol., 147, 539–560, https://doi.org/10.1046/j.1469-8137.2000.00712.x, 2000.

Hanson, P. J. and Lindberg, S. E.: Dry Deposition of Reactive Nitrogen-Compounds – a Review of Leaf, Canopy and Non-Foliar Measurements, Atmos. Environ. A-Gen., 25, 1615–1634, https://doi.org/10.1016/0960-1686(91)90020-8, 1991.

Hereid, D. P. and Monson, R. K.: Nitrogen oxide fluxes between corn (Zea mays L.) leaves and the atmosphere, Atmos. Environ., 35, 975–983, https://doi.org/10.1016/S1352-2310(00)00342-3, 2001.

Jacob, D. J. and Wofsy, S. C.: Budgets of Reactive Nitrogen, Hydrocarbons, and Ozone over the Amazon-Forest during the Wet Season, J. Geophys. Res.-Atmos., 95, 16737–16754, https://doi.org/10.1029/JD095iD10p16737, 1990.

Johansson, C.: Pine forest: a negligible sink for atmospheric NO_x in rural Sweden, Tellus B, 39B, 426–438, 1987.

Lee, Y. N. and Schwartz, S. E.: Evaluation of the Rate of Uptake of Nitrogen-Dioxide by Atmospheric and Surface Liquid Water, J. Geophys. Res.-Oceans, 86, 1971–1983, https://doi.org/10.1029/JC086iC12p11971, 1981a.

Lee, Y. N. and Schwartz, S. E.: Reaction-Kinetics of Nitrogen-Dioxide with Liquid Water at Low Partial-Pressure, J. Phys. Chem.-US, 85, 840–848, https://doi.org/10.1021/j150607a022, 1981b.

Lerdau, M. T., Munger, L. J., and Jacob, D. J.: Atmospheric chemistry – The NO_2 flux conundrum, Science, 289, 2291–2293, https://doi.org/10.1126/science.289.5488.2291, 2000.

Matsumoto, J. and Kajii, Y.: Improved analyzer for nitrogen dioxide by laser-induced fluorescence technique, Atmos. Environ., 37, 4847–4851, https://doi.org/10.1016/j.atmosenv.2003.08.023, 2003.

Mckenney, D. J., Shuttleworth, K. F., Vriesacker, J. R., and Findlay, W. I.: Production and Loss of Nitric-Oxide from Denitrification in Anaerobic Brookston Clay, Appl. Environ. Microb., 43, 534–541, 1982.

Meixner, F. X., Fickinger, T., Marufu, L., Serca, D., Nathaus, F. J., Makina, E., Mukurumbira, L., and Andreae, M. O.: Preliminary results on nitric oxide emission from a southern African savanna ecosystem, Nutr. Cycl. Agroecosys., 48, 123–138, 1997.

Min, K.-E., Pusede, S. E., Browne, E. C., LaFranchi, B. W., Wooldridge, P. J., Wolfe, G. M., Harrold, S. A., Thornton, J. A., and Cohen, R. C.: Observations of atmosphere-biosphere exchange of total and speciated peroxynitrates: nitrogen fluxes and biogenic sources of peroxynitrates, Atmos. Chem. Phys., 12, 9763–9773, https://doi.org/10.5194/acp-12-9763-2012, 2012.

Min, K.-E., Pusede, S. E., Browne, E. C., LaFranchi, B. W., and Cohen, R. C.: Eddy covariance fluxes and vertical concentration gradient measurements of NO and NO_2 over a ponderosa pine ecosystem: observational evidence for within-canopy chemical removal of NO_x, Atmos. Chem. Phys., 14, 5495–5512, https://doi.org/10.5194/acp-14-5495-2014, 2014.

Neubert, A., Kley, D., Wildt, J., Segschneider, H. J., and Forstel, H.: Uptake of NO, NO_2 and O_3 by Sunflower (Helianthus-Annuus L) and Tobacco Plants (Nicotiana-Tabacum-L) – Dependence on Stomatal Conductivity, Atmos. Environ. A-Gen., 27, 2137–2145, https://doi.org/10.1016/0960-1686(93)90043-X, 1993.

Nussbaum, S., Vonballmoos, P., Gfeller, H., Schlunegger, U. P., Fuhrer, J., Rhodes, D., and Brunold, C.: Incorporation of Atmospheric (NO_2)-N-15-Nitrogen into Free Amino-Acids by Norway Spruce Picea-Abies (L) Karst, Oecologia, 94, 408–414, https://doi.org/10.1007/Bf00317117, 1993.

Okano, K. and Totsuka, T.: Absorption of Nitrogen-Dioxide by Sunflower Plants Grown at Various Levels of Nitrate, New Phytol., 102, 551–562, https://doi.org/10.1111/j.1469-8137.1986.tb00831.x, 1986.

Pape, L., Ammann, C., Nyfeler-Brunner, A., Spirig, C., Hens, K., and Meixner, F. X.: An automated dynamic chamber system for surface exchange measurement of non-reactive and reactive trace gases of grassland ecosystems, Biogeosciences, 6, 405–429, https://doi.org/10.5194/bg-6-405-2009, 2009.

Ramge, P., Badeck, F. W., Plochl, M., and Kohlmaier, G. H.: Apoplastic Antioxidants as Decisive Elimination Factors within the Uptake Process of Nitrogen-Dioxide into Leaf Tissues, New Phytol., 125, 771–785, https://doi.org/10.1111/j.1469-8137.1993.tb03927.x, 1993.

Reed, C., Evans, M. J., Di Carlo, P., Lee, J. D., and Carpenter, L. J.: Interferences in photolytic NO2 measurements: explanation for an apparent missing oxidant?, Atmos. Chem. Phys., 16, 4707–4724, https://doi.org/10.5194/acp-16-4707-2016, 2016.

Rogers, H. H., Jeffries, H. E., and Witherspoon, A. M.: Measuring Air Pollutant Uptake by Plants – Nitrogen-Dioxide, J. Environ. Qual., 8, 551–557, https://doi.org/10.2134/jeq1979.00472425000800040022x, 1979.

Rondon, A., Johansson, C., and Granat, L.: Dry Deposition of Nitrogen-Dioxide and Ozone to Coniferous Forests, J. Geophys. Res.-Atmos., 98, 5159–5172, https://doi.org/10.1029/92jd02335, 1993.

Rondon, A. and Granat, L.: Studies on the Dry Deposition of NO_2 to Coniferous Species at Low NO_2 Concentrations, Tellus B, 46, 339–352, https://doi.org/10.1034/j.1600-0889.1994.t01-4-00001.x, 1994.

Schneider, C. A., Rasband, W. S., and Eliceiri, K. W.: NIH Image to ImageJ: 25 years of image analysis, Nat. Methods, 9, 671–675, https://doi.org/10.1038/nmeth.2089, 2012.

Seinfeld, J. H. and Pandis, S. N.: Atmospheric Chemistry and Physics: From Air Pollution to Global Change, 2nd edn., Wiley, New York, 2006.

Seok, B., Helmig, D., Ganzeveld, L., Williams, M. W., and Vogel, C. S.: Dynamics of nitrogen oxides and ozone above and within a mixed hardwood forest in northern Michigan, Atmos. Chem. Phys., 13, 7301–7320, https://doi.org/10.5194/acp-13-7301-2013, 2013.

Sparks, J. P., Monson, R. K., Sparks, K. L., and Lerdau, M.: Leaf uptake of nitrogen dioxide (NO_2) in a tropical wet forest: implications for tropospheric chemistry, Oecologia, 127, 214–221, https://doi.org/10.1007/s004420000594, 2001.

Teklemariam, T. A. and Sparks, J. P.: Leaf fluxes of NO and NO_2 in four herbaceous plant species: The role of ascorbic acid, Atmos. Environ., 40, 2235–2244, https://doi.org/10.1016/j.atmosenv.2005.12.010, 2006.

Thoene, B., Schroder, P., Papen, H., Egger, A., and Rennenberg, H.: Absorption of Atmospheric No2 by Spruce (Picea-Abies L Karst) Trees 1, NO_2 Influx and Its Correlation with Nitrate Reduction, New Phytol., 117, 575–585, https://doi.org/10.1111/j.1469-8137.1991.tb00962.x, 1991.

Thornton, J. A., Wooldridge, P. J., and Cohen, R. C.: Atmospheric NO2: In situ laser-induced fluorescence detection at parts per trillion mixing ratios, Anal. Chem., 72, 528–539, https://doi.org/10.1021/ac9908905, 2000.

Tischner, R.: Nitrate uptake and reduction in higher and lower plants, Plant Cell Environ., 23, 1005–1024, https://doi.org/10.1046/j.1365-3040.2000.00595.x, 2000.

Vinken, G. C. M., Boersma, K. F., Maasakkers, J. D., Adon, M., and Martin, R. V.: Worldwide biogenic soil NO_x emissions inferred from OMI NO_2 observations, Atmos. Chem. Phys., 14, 10363–10381, https://doi.org/10.5194/acp-14-10363-2014, 2014.

von Caemmerer, S. and Farquhar, G. D.: Some Relationships between the Biochemistry of Photosynthesis and the Gas-Exchange of Leaves, Planta, 153, 376–387, 1981.

Wang, Y. P. and Leuning, R.: A two-leaf model for canopy conductance, photosynthesis and partitioning of available energy I: Model description and comparison with a multi-layered model, Agr. Forest Meteorol., 91, 89–111, https://doi.org/10.1016/S0168-1923(98)00061-6, 1998.

Weber, P., Nussbaum, S., Fuhrer, J., Gfeller, H., Schlunegger, U. P., Brunold, C., and Rennenberg, H.: Uptake of Atmospheric (NO_2)-N-15 and Its Incorporation into Free Amino-Acids in Wheat (Triticum-Aestivum), Physiol. Plantarum, 94, 71–77, https://doi.org/10.1034/j.1399-3054.1995.940111.x, 1995.

Wildt, J., Kley, D., Rockel, A., Rockel, P., and Segschneider, H. J.: Emission of NO from several higher plant species, J. Geophys. Res.-Atmos., 102, 5919–5927, https://doi.org/10.1029/96jd02968, 1997.

Wolfe, G. M. and Thornton, J. A.: The Chemistry of Atmosphere-Forest Exchange (CAFE) Model – Part 1: Model description and characterization, Atmos. Chem. Phys., 11, 77–101, https://doi.org/10.5194/acp-11-77-2011, 2011.

Yienger, J. J. and Levy, H.: Empirical-Model of Global Soil-Biogenic NO_x Emissions, J. Geophys. Res.-Atmos., 100, 11447–11464, https://doi.org/10.1029/95jd00370, 1995.

Yoneyame, T., Ito, O., and Engelaar, W. M. H. G.: Uptake, metabolism and distribution of nitrogen in crop plants traced by enriched and natural 15N: Progress over the last 30 years, Phytochem. Rev., 2, 121–132, https://doi.org/10.1023/B:PHYT.0000004198.95836.ad, 2003.